Journal of Natural Medicines
https://doi.org/10.1007/s11418-023-01706-w

ORIGINAL PAPER

Antimalarial ceramicines Q-T from *Chisocheton ceramicus*

Alfarius Eko Nugroho[1] · Chin Piow Wong[1] · Yusuke Hirasawa[1] · Toshio Kaneda[1] · Takahiro Tougan[2] · Toshihiro Horii[3] · A. Hamid A. Hadi[4] · Hiroshi Morita[1]

Received: 9 March 2023 / Accepted: 29 April 2023

Abstract

Ceramicines are a series of limonoids that were isolated from the bark of Malaysian *Chisocheton ceramicus* (Meliaceae) and were known to show various biological activity. Four new limonoids, ceramicines Q–T (**1–4**) were isolated from the barks of *C. ceramicus*, and their structures were determined on the basis of the 1D and 2D NMR analyses in combination with calculated ^{13}C chemical shift data. Ceramicines Q–T (**1–4**) were established to be new limonoids with a cyclopentanone[α] phenanthren ring system with a β-furyl ring at C-17, and without a tetrahydrofuran ring like ceramicine B, which is characteristic of known ceramicines. Ceramicine R (**2**) exhibited potent antimalarial activity against *Plasmodium falciparum* 3D7 strain with IC_{50} value of 2.8 μM.

Graphical abstract

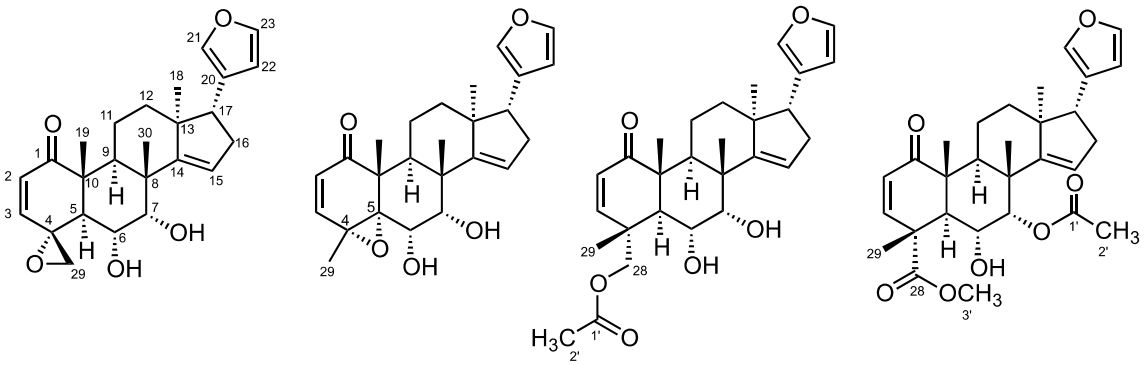

Keywords Ceramicines Q–T · Limonoids · *Chisocheton ceramicus* · Meliaceae · Antimalarial activity

✉ Yusuke Hirasawa
y-hirasawa@hoshi.ac.jp

✉ Hiroshi Morita
moritah@hoshi.ac.jp

1 Faculty of Pharmaceutical Sciences, Hoshi University, Ebara 2-4-41 Shinagawa-ku, Tokyo 142-8501, Japan

2 Department of Cellular Immunology, Research Institute for Microbial Diseases, Osaka University, 3–1 Yamadaoka, Suita, Osaka 565–0871, Japan

3 Department of Malaria Vaccine Development, Research Institute for Microbial Diseases, Osaka University, 3-1 Yamadaoka, Suita, Osaka 565-0871, Japan

4 Department of Chemistry, Faculty of Science, University of Malaya, 50603 Kuala Lumpur, Malaysia

Introduction

The plants belonging to Meliaceae have been reported to produce limonoids [1]. In our search for new bioactive compounds from medicinal plants, we have reported the isolation of new limonoids from plants of this genus [2–15], and alkaloids [16–23] and coumarins [24] showing antimalarial activity or inhibiting acetylcholinesterase. Ceramicine B, in particular, has been reported to show a strong lipid droplets accumulation (LDA) inhibitory activity on mouse pre-adipocyte cell line (MC3T3-G2/PA6) [6–8] and also anti-melanin deposition activity [9]. With the purpose of

Published online: 10 May 2023

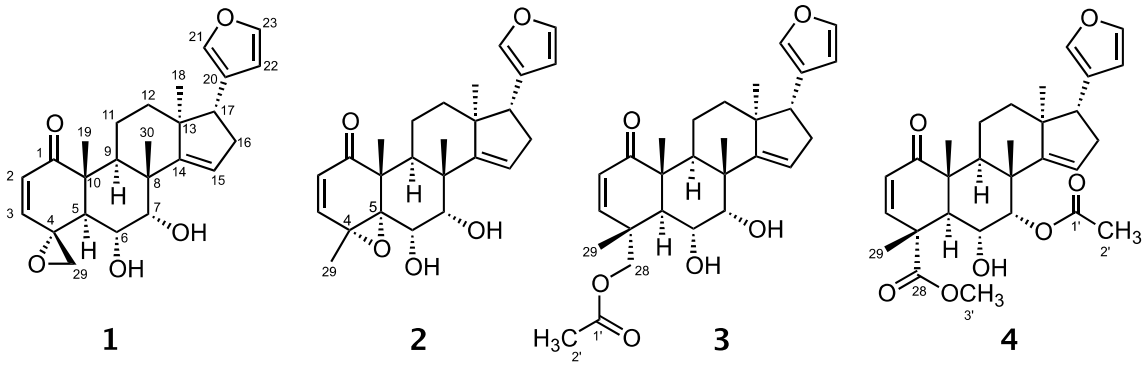

Fig. 1 Structures of **1**–**4**

Table 1 ^{1}H and ^{13}C NMR data of **1** and **2** in $CDCl_3$

No.	**1**		**2**	
	δ_H(J, Hz)	δ_C	δ_H(J, Hz)	δ_C
1		202.0		199.5
2	5.98 (1H, d, 10.2)	131.0	5.94 (1H, d, 10.0)	129.9
3	6.23 (1H, d, 10.2)	146.7	6.70 (1H, d, 10.0)	148.2
4		60.4		55.6
5	3.01 (1H, d, 10.8)	43.5		68.0[a]
6	4.12 (1H, dd, 10.8, 2.4)	66.7	4.50 (1H, m)	63.8
7	3.92 (1H, d, 2.4)	74.3	4.12 (1H, brd, 2.7)	77.7
8		43.3		43.6
9	2.69 (1H, dd, 11.8, 5.8)	32.5	2.85 (1H, m)	29.7
10		50.3		50.3
11a	1.56 (1H, m)	17.8	1.61 (1H, m)	18.5
11b	2.51 (1H, m)		2.47 (1H, m)	
12a	1.63 (1H, m)	33.2	1.61 (1H, m)	32.6
12b	1.93 (1H, m)		1.94 (1H, m)	
13		47.0		47.2
14		159.6		160.0[a]
15	5.54 (1H, brd, 2.0)	119.6	5.60 (1H, brd, 2.0)	119.9
16a	2.39 (1H, ddd, 15.2, 7.3, 3.4)	34.4	2.42 (1H, ddd, 15.4, 7.2, 3.4)	34.3
16b	2.56 (1H, dd, 15.2, 11.5)		2.57 (1H, dd, 15.4, 11.0)	
17	2.85 (1H, dd, 11.5, 7.3)	62.0	2.88 (1H, m)	52.1
18	0.92 (3H, s)	21.5	0.94 (3H, s)	21.2
19	1.31 (3H, s)	14.8	1.32 (3H, s)	19.2
20		124.6		124.4
21	7.25 (1H, brs)	139.7	7.26 (1H, m)	139.7
22	6.30 (1H, brs)	111.1	6.29 (1H, brs)	111.0
23	7.37 (1H, brt, 1.8)	142.5	7.39 (1H, brt, 1.6)	142.7
29a	3.09 (1H, d, 3.5)	60.4	1.86 (1H, s)	18.4
29b	3.65 (1H, d, 3.6)			
30	1.17 (3H, s)	26.2	1.29 (3H, s)	25.8

[a]Based on HMBC correlations

discovering limonoids with biological activity, we further investigated the constituents of *C. ceramicus* which led to the isolation of four new limonoids, ceramicines Q–T (**1–4**), and ceramicine R (**2**) showed potent antimalarial activity

Table 2 ^{1}H and ^{13}C NMR data of **3** and **4** in $CDCl_3$

No.	**3**		**4**	
	δ_H(J, Hz)	δ_C	δ_H(J, Hz)	δ_C
1		204.7		203.2
2	5.80 (1H, d, 10.2)	126.0	5.86 (1H, d, 10.1)	126.9
3	6.27 (1H, m)	151.3	6.32 (1H, d, 10.1)	146.4
4		40.9		47.7
5	2.38 (1H, d, 11.2)	41.7	3.27 (1H, d, 11.8)	44.0
6	4.20 (1H, brd, 11.2)	67.9	4.23 (1H, m)	66.5
7	3.94 (1H, brd, 2.2)	76.0	5.35 (1H, brd, 2.2)	78.5
8		44.0		42.8
9	2.47 (1H, m)	33.1	2.57 (1H, dd, 11.5, 4.9)	35.3
10		49.2		48.3
11a	1.52 (1H, m)	17.6	1.57 (1H, m)	18.5
11b	2.47 (1H, m)		2.47 (1H, m)	
12a	1.57 (1H, m)	32.8	1.66 (1H, m)	33.7
12b	1.90 (1H, m)		1.94 (1H, m)	
13		47.1		47.0
14		161.0		158.4
15	5.55 (1H, brd, 2.2)	119.8	5.43 (1H, m)	120.0
16a	2.42 (1H, m)	34.3	2.34 (1H, m)	34.3
16b	2.53 (1H, m)		2.39 (1H, m)	
17	2.85 (1H, dd, 10.8, 7.4)	51.9	2.83 (1H, dd, 10.5, 7.7)	52.0
18	0.90 (3H, s)	21.3	0.89 (3H, s)	22.2
19	1.32 (3H, s)	17.0	1.30 (3H, s)	16.3
20		124.4		124.7
21	7.25 (1H, brs)	139.7	7.24 (1H, brs)	139.7
22	6.28 (1H, m)	111.0	6.29 (1H, brs)	111.0
23	7.38 (1H, brs)	142.6	7.38 (1H, brt, 1.5)	142.6
28a	4.03 (1H, d, 10.8)	72.0		175.8
28b	4.59 (1H, d, 10.8)			
29a	1.36 (3H, s)	17.0	1.61 (3H, s)	17.0
29b				
30	1.19 (3H, s)	26.6	1.26 (3H, s)	26.7
1’		171.3		171.8
2’	2.01 (3H, s)	21.0	2.04 (3H, s)	21.0
3’			3.65 (3H, s)	52.7

(Fig. 1). Their structures were determined on the basis of NMR and MS spectroscopic analyses in combination with NMR chemical shifts calculations.

Results and discussions

Compounds **1**–**4** were obtained as optically active white amorphous solids. The ^{1}H and ^{13}C NMR data (Tables 1 and 2) suggested the identity of **1**–**4** as ceramicine derivatives.

Ceramicine Q (**1**) was obtained as an optically active, $[\alpha]_D^{27}+119$ (*c* 1.0, $CHCl_3$), white amorphous solid and was revealed to have the molecular formula $C_{25}H_{30}O_5$, by HRESITOFMS [*m/z* 433.1991 $(M+Na)^+$, $\Delta-1.4$ mmu]. IR absorptions implied the presence of α,β-unsaturated ketone (1683 cm^{-1}) and hydroxy (3461 cm^{-1}) groups. ^{1}H and ^{13}C NMR data (Table 1) revealed 25 carbon resonances due to one carbonyl, two sp^2 quaternary carbons, four sp^3 quaternary carbons, six sp^2 methines, five sp^3 methines, four sp^3 methylenes, and three methyls. Among them, four sp^3 carbons (δ_C60.4, 60.4, 66.7, and 74.3) and two sp^2 methines (δ_C 139.7 and 142.5) were ascribed to those bearing an oxygen atom.

Analyses of the HSQC and ^{1}H-^{1}H COSY spectra (Fig. 2) revealed the presence of four partial structures; **a** (C-2 and C-3), **b** (C-5 ~ C-7), **c** (C-9, C-11, and C-12), **d** (C-15 ~ C-17), and **e** (C-22 ~ C-23). HMBC correlations of H_3-18 to C-12, C-13, C-14 and C-17 suggested the connectivity of **c**, **d**, and C-14 through C-13. HMBC correlations of H-17 to C-21, H-16 to C-20, and H-23 to C-20 and C-21 suggested the presence of β-furyl at C-17, and the correlation of H_2-16 to C-13 and C-14 completed the structure of ring D. The presence of ring C was deduced from the HMBC cross-peaks of H_3-30 to C-7, C-8, C-9 and C-14, and the connectivity of **b**, C-1, C-5, and C-19 through C-10 was suggested by the HMBC correlations of H_3-19 to C-1, C-5, C-9 and C-10. HMBC correlations of H-2 to C-10 and C-4, and H-3 to C-1 and C-5 suggested the presence of ring A. Finally, HMBC correlations of H-3 to C-29 (δ_C 60.4) suggested the presence of 1-oxaspiro[2.5]oct-4-ene of **1** as shown in Fig. 2.

The relative configuration of **1** was assigned by analyses of the ^{1}H-^{1}H coupling constant data and the NOESY correlations (Fig. 2). First, H-6, H-17, CH_3-19, and CH_3-30 were assigned to be *β*-axially oriented from the NOESY correlations of H-6/H_3-19 and H_3-30/H-17 and H_3-19, while H-5, H-9 and CH_3-18 were deduced to possess *α*-orientation from the NOESY correlations of H-9/H-5 and H_3-18. Both H-6 and H-7 should possess β-orientation because of the multiplicity pattern of H-6 (dd, 10.8, 2.4) and H-7 (d, 2.4). The stereochemistry of epoxy ring was elucidated to be as shown in Fig. 2 by the presence of NOESY correlations of H-29a/H-3 and H_3-19, and H-29b/H_3-19.

Ceramicine R (**2**), $[\alpha]_D^{28}$ 126 (*c* 0.5, $CHCl_3$), was revealed to have the molecular formula $C_{25}H_{30}O_5$ by HRESITOFMS. Its NMR data are highly similar to **1**. However, the signals for oxymethylene of H_2-29 in **1** are not observed in **2**, and a methyl signal (δ_H 1.86) and two sp^3 quaternary carbons bearing an oxygen atom (δ_C 55.6 and 68.0) are observed instead. Analysis of the 2D NMR data including HMBC and NOESY (Fig. 3) correlations supported the structure of **2** to be 4,5-epoxy derivative as shown in Fig. 1. Specifically, the HMBC correlations of H_3-29 to C-3, C-4 (δ_C 55.6) and C-5 (δ_C 68.0), and H_3-19 to C-5 supported its functionality in the structure of **2**.

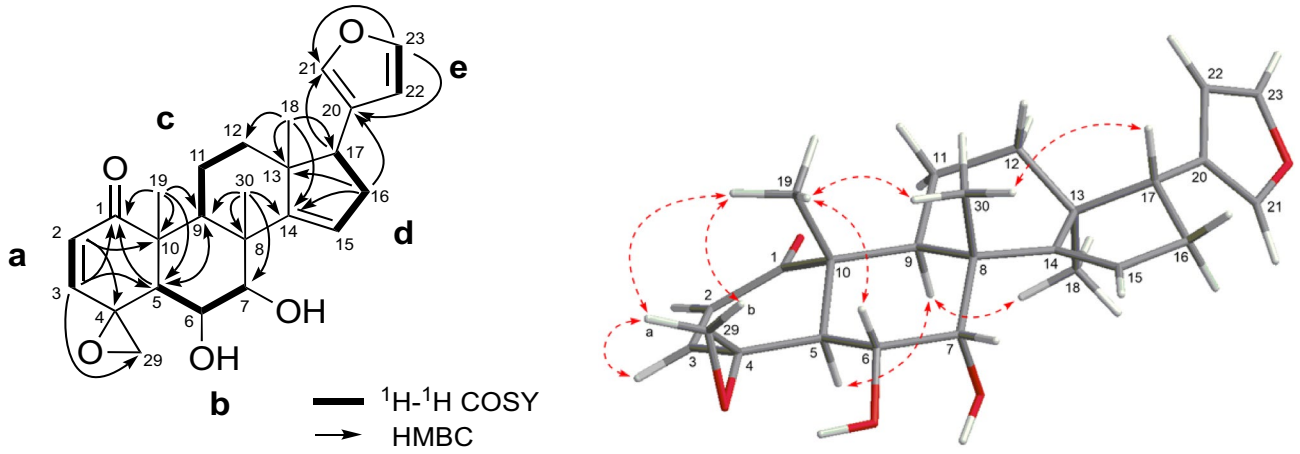

Fig. 2 Selected 2D NMR correlations of **1**

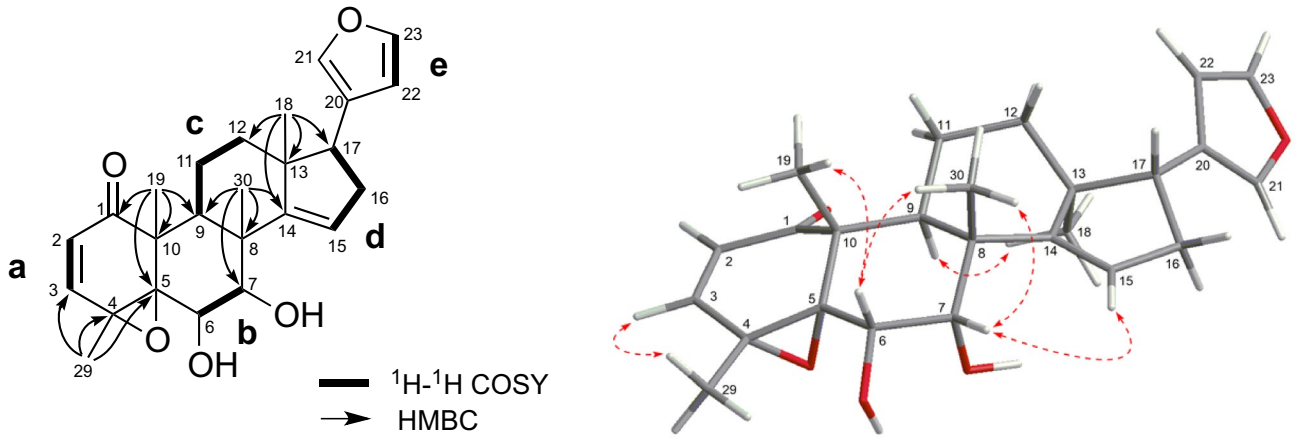

Fig. 3 Selected 2D NMR correlations of **2**

NOESY correlations of H-6/H_3-19 and H_3-30, H-7/H_3-30 and H-15, and H-9/H_3-18 supported the stereochemistry of **2**. Configurations of H-6 and H-7 taking β-orientation like as in **1** also supported by proton ^3J coupling constant ($J = 2.7$ Hz).

The remaining problem regarding stereochemistry is that of epoxy in positions 4 and 5. Only the presence of two NOESY correlations of H-3/H_3-29 and H-6/H_3-19 is difficult to determine unequivocally. Therefore, we compared the predicted NMR chemical shifts of the two possible diastereomers, **2a** (4,5-α-epoxy) and **2b** (4,5-β-epoxy) as shown below (Fig. 4), calculated for the ωB97X-V/6-311+G* optimized conformations using ωB97X-V/6-311+G*(2df,2p).

Conformational searches and chemical shift calculations for compounds **2a** and **2b** were performed with the Spartan'20 software [25]. Stable conformers up to 40 kJ/mol for **2a** and **2b** were initially searched using the Merck molecular force field (MMFF) method. Stable conformers suggested were optimized using Hartree–Fock (HF)/3-21G (40 kJ/mol) and ωB97X-D/6-31G* (15 kJ/mol). Final energy optimization for the Boltzmann distribution was conducted at the ωB97X-V/6-311+G*(2df,2p) level of theory. NMR properties were calculated at the ωB97X-V/6-311+G*(2df,2p) level of theory and scaled. The obtained chemical shifts were corrected using the Boltzmann distribution to give calculated ^{13}C chemical shifts.

The ^{13}C chemical shift differences of predicted and experimental data are shown as graph in Fig. 5. Two atoms of C-6 and C-9 in **2b** shows a deviation of greater than 5 ppm, but the average deviation is less than 2 ppm in **2a**. Overall, the ^{13}C chemical shifts predicted for structure **2a** (Fig. 4) correlate very well with those observed for ceramicine R (**2**).

Thus, we propose that the correct structure of ceramicine R (**2**) is the structure **2a**. The prediction of ^{13}C chemical shifts by DFT calculation is a very powerful tool for

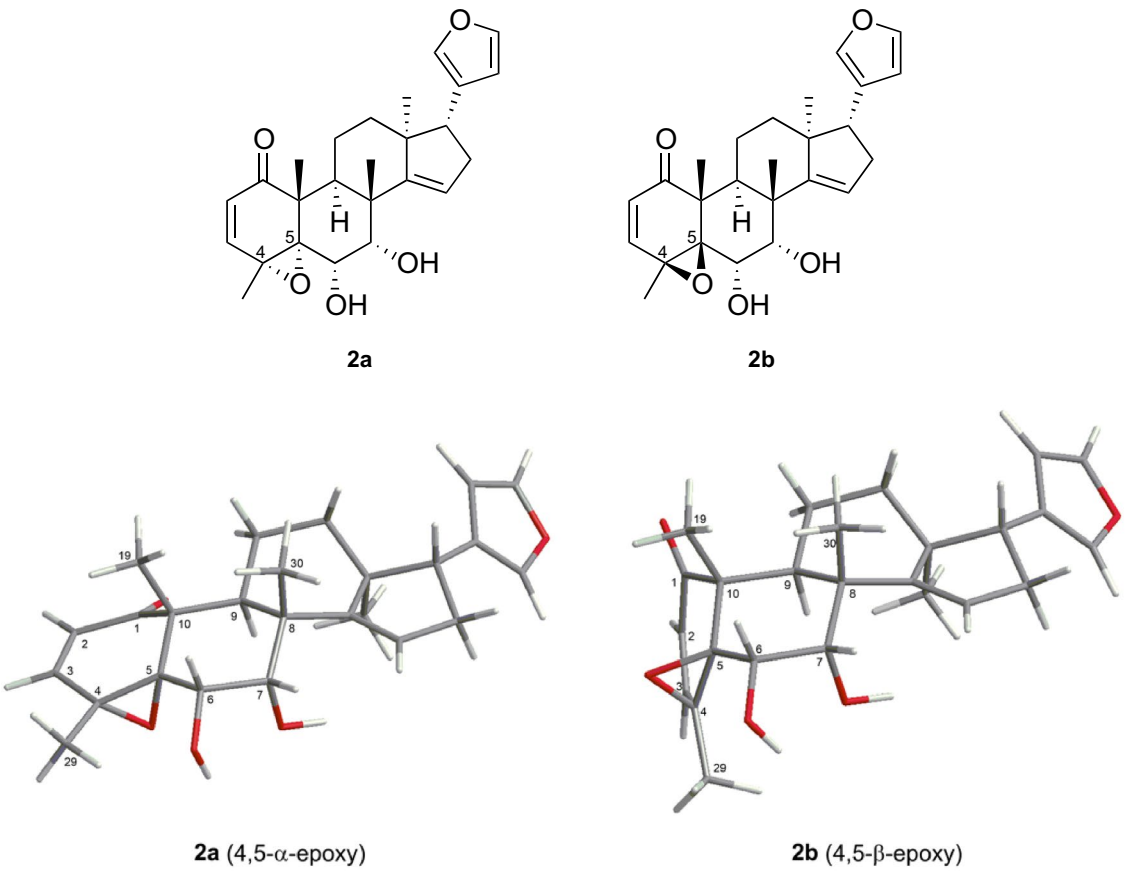

Fig. 4 Structures of the lowest-energy conformation of the two possible isomers (**2a** and **2b**) of ceramicine R (**2**)

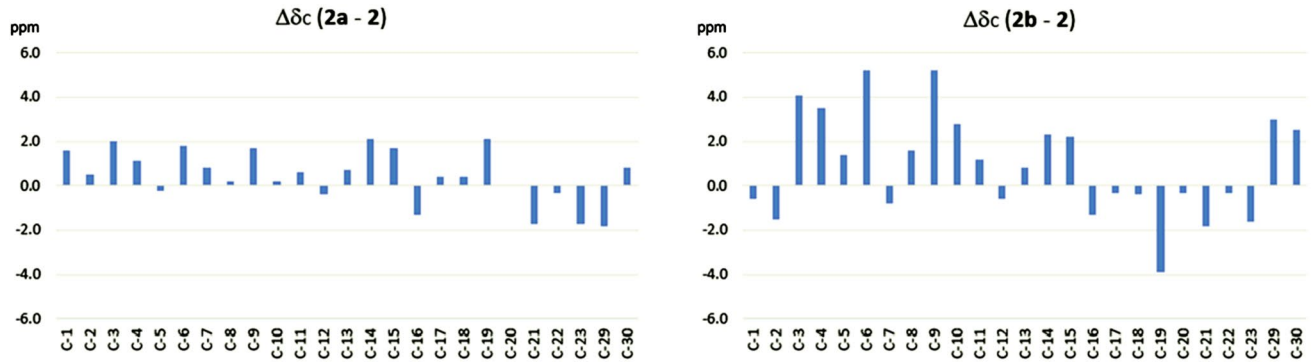

Fig. 5 Parts per million difference between the calculated ^{13}C NMR shifts for the two possible isomers (**2a** and **2b**) and the experimental data of ceramicine R (**2**)

screening proposed structures and should be used more widely.

Ceramicine S (**3**), $[\alpha]_D^{27} + 34$ (*c* 1.0, $CHCl_3$), was revealed to have the molecular formula $C_{28}H_{36}O_6$ by HRESITOFMS. Its ^1H and ^{13}C NMR data are highly similar to ceramicine R (**2**) (Table 2). However, the NMR data of **3** suggested that the oxymethylene moiety [δ_H 4.03 (d, 10.8), 4.59 (d, 10.8); δ_C 72.0] with acetyl group [δ_H 2.01 (3H, s); δ_C 21.0 and

171.3] was observed instead of the epoxide function in **2**. IR absorptions implied the presence of *α,β*-unsaturated ketone (1684 cm^{-1}), hydroxy (3502 cm^{-1}), and acetyl (1733 cm^{-1}) groups. The HMBC correlations of H_2-28 and H_3-2' to C-1' (δ_C 171.3) supported its functionality in the structure of **3**. Finally, the NOESY correlations confirmed the position of the oxymethylene moiety with the acetyl group at C-28 and the α orientation of the hydroxy at C-6 and C-7 (See Supplementary Information).

By HRESITOFMS, ceramicine T (**4**), $[\alpha]_D^{28} + 67$ (*c* 0.5, $CHCl_3$), was revealed to have the molecular formula $C_{29}H_{36}O_7$. Their NMR data are also highly similar to **3**, differing only on the signals assigned to the presence of one acetyl and one methoxy carbonyl groups in **4** and the disappearance of oxy-methylene protons of **3**. IR absorptions implied the presence of *α,β*-unsaturated ketone (1683 cm^{-1}), hydroxy (3534 cm^{-1}), and acetyl and/or methoxycarbonyl (1732 cm^{-1}) groups. Analysis of the NMR data revealed the presence of a cyclopentanone[α]phenanthren ring system with a β-furyl ring at C-17.

The planar structure of **4** was deduced from the ^1H-^1H COSY correlations and the especially HMBC correlations of H_3-29 and H_3-3' to C-28 and H_3-30 to C-7. The relative configuration of **4** was then deduced from the NOESY correlations of H-6/H_3-19, H_3-29 and H_3-30, H-9/H-5 and H_3-18, H-7/H_3-30, and H-12a/H_3-30 and H-17 (See Supplementary Information). Thus, the structure of **4** was proposed to be as shown in Fig. 1.

Considering that **1**–**4** were isolated from the same extract as ceramicine B [3], their absolute configurations were assumed to be similar to ceramicine B based on the biogenetic relationships. Ceramicines Q and R might be generated from a cyclopentanone[α]phenanthren ring system followed by oxidative decarboxylation at C-28.

Antimalarial activity

Ceramicines Q–T (**1–4**) were tested for antimalarial activity against *Plasmodium falciparum* 3D7 strain. The assay showed that **2** had potent in vitro antimalarial activity [the half-maximal (50%) inhibitory concentration (IC_{50}) = 2.8 μM, whereas **1**, **3**, and **4** did not (> 5.0 μM).].

Previously, we also reported some limonoids, ceramicines A–D with a cyclopentanone[α]phenanthren ring system with a tetrahydrofuran ring and a β-furyl ring from the barks of *C. ceramicus*, exhibited antimalarial activity against *P. falciparum* 3D7 in vitro [2, 3].

The activity might be depending on their unique cyclopentanone[α]phenanthren ring system and also be influenced by the presence of a tetrahydrofuran ring and its substituent patterns around rings A and B.

Experimental section

General experimental procedures

Optical rotations were measured on a JASCO DIP-1000 polarimeter. UV spectra were recorded on a Shimadzu UVmini-1240 spectrophotometer and IR spectra on a JASCO FT/IR-4100 spectrophotometer. High-resolution ESI MS were obtained on a JMS-T100LP (JEOL). ^1H and 2D NMR spectra were measured on a 400 MHz or 600 MHz spectrometer at 300 K, while ^{13}C NMR spectra were on a 100 MHz or 150 MHz spectrometer. The residual solvent peaks were used as internal standards (δ_H 7.26 and δ_C 77.0 for $CDCl_3$, δ_H 3.31 and δ_C 49.0 for CD_3OD).

Material

The barks of *C. ceramicus* were collected in Terengganu, Malaysia in July 2013. The botanical identification was made by Prof. A. Hamid A. Hadi, University of Malaya. Voucher specimens (No. HOSHI13CCB) are deposited in the department of Pharmacognosy Hoshi University.

Extraction and isolation

The barks of *C. ceramicus* (8 kg) were extracted with MeOH to obtain 1.43 kg of extract. The MeOH extract was successively partitioned with *n*-hexane, EtOAc, *n*-BuOH and water. The *n*-hexane-soluble materials were separated further by silica gel column chromatography (*n*-hexane/EtOAc 1:0→1:1, $CHCl_3$/MeOH 1:0→0:1) to obtain 10 fractions (A–J). Fraction I was separated further with a ODS silica gel column (MeOH/H_2O 7:3→1:0, acetone) to obtain 6 fractions (I-1–I-6). Fraction I-3 was also separated by HPLC (Shiseido ODS MGII 30 × 250 mm, 85% aqueous MeOH at 8.0 mL/min, UV detection at 210 nm) into 7 fractions (I-3-a–I-3-g). Fraction I-3-c, I-3-d, and I-3-f are ceramicine F, G and B, respectively. Separation of fraction I-3-a by HPLC (Nacalai tesque Cholester 10 × 250 mm, 65% aqueous MeCN at 2.0 mL/min, UV detection at 210 nm) yielded ceramicine Q (**1**) (6.0 mg, 0.000075%, t_R 18.6 min) and ceramicine R (**2**) (0.8 mg, 0.00001%, t_R 21.0 min).

Separation of fraction I-3-e by HPLC (Nacalai tesque Cholester 10 × 250 mm, 60% aqueous MeCN at 2.0 mL/min, UV detection at 210 nm) yielded ceramicine S (**3**) (10.6 mg, 0.00013%, t_R 44.0 min) and ceramicine T (**4**) (1.0 mg, 0.000012%, t_R 50.0 min).

Ceramicine Q (1): white amorphous solid; $[\alpha]_D^{27} + 119$ (*c* 1.0, $CHCl_3$); UV (MeOH) λ_{max} (ε) 204 (10,000) nm; CD (MeOH) λ_{max} ($\Delta\varepsilon$) 337 (− 1.59) and 216 (10.3) nm; IR (Zn-Se) ν_{max} 3461 and 1683 cm^{-1}; ^1H and ^{13}C NMR data (Table 1); ESIMS *m/z* 433 $(M + Na)^+$; HRESIMS *m/z*

433.1977 $(M+Na)^+$ [calcd for $C_{25}H_{30}O_5Na$ $(M+Na)^+$: 433.1991].

Ceramicine R (2): white amorphous solid; $[\alpha]_D^{28}+126$ (*c* 0.5, $CHCl_3$); UV (MeOH) λ_{max} (ε) 204 (10,700) nm; CD (MeOH) λ_{max} ($\Delta\varepsilon$) 336 (− 2.36), 250 (2.18) and 230 (1.52) nm; IR (Zn-Se) ν_{max} 3450 and 1697 cm^{-1}; ^1H and ^{13}C NMR data (Table 1); ESIMS *m/z* 433 $(M+Na)^+$; HRESIMS *m/z* 433.1982 $(M+Na)^+$ [calcd for $C_{25}H_{30}O_5Na$ $(M+Na)^+$: 433.1991].

Ceramicine S (3): white amorphous solid; $[\alpha]_D^{27}+34$ (*c* 1.0, $CHCl_3$); UV (MeOH) λ_{max} (ε) 204 (11,900) nm; CD (MeOH) λ_{max} ($\Delta\varepsilon$) 333 (− 2.96), 249 (Δ 0.36), 230 (Δ − 0.35) and 212 (Δ 3.79) nm; IR (Zn-Se) ν_{max} 3502, 1733 and 1684 cm^{-1}; ^1H and ^{13}C NMR data (Table 1); ESIMS *m/z* 491 $(M+Na)^+$; HRESIMS *m/z* 491.2417 $(M+Na)^+$ [calcd for $C_{28}H_{36}O_6Na$ $(M+Na)^+$: 491.2410].

Ceramicine T (4): white amorphous solid; $[\alpha]_D^{28}+67$ (*c* 0.5, $CHCl_3$); UV (MeOH) λ_{max} (ε) 204 (12,000) nm; CD (MeOH) λ_{max} ($\Delta\varepsilon$) 336 (− 2.21), 234 (− 12.6), 206 (17.0) nm; IR (Zn-Se) ν_{max} 3534, 1732 and 1683 cm^{-1}; ^1H and ^{13}C NMR data (Table 2); ESIMS *m/z* 519 $(M+Na)^+$; HRESIMS *m/z* 519.2361 $(M+Na)^+$ [calcd for $C_{29}H_{36}O_7Na$ $(M+Na)^+$: 519.2359].

^{13}C chemical shift calculations

Conformational searches and chemical shift calculations for compounds **2a** and **2b** were performed with the Spartan'20 software [25]. Stable conformers up to 40 kJ/mol for **2a** and **2b** were initially searched using the Merck molecular force field (MMFF) method. Stable conformers suggested were optimized using Hartree–Fock (HF)/3-21G (40 kJ/mol) and ωB97X-D/6-31G* (15 kJ/mol). Final energy optimization for the Boltzmann distribution was conducted at the ωB97X-V/6-311+G*(2df,2p) level of theory. NMR properties were calculated at the ωB97X-V/6-311+G*(2df,2p) level of theory and scaled. The obtained chemical shifts were corrected using the Boltzmann distribution to give calculated ^{13}C chemical shifts.

Parasite strain culture

P. falciparum laboratory strain 3D7 was obtained from Prof. Masatsugu Kimura (Osaka City University, Osaka, Japan). For the assessment of antimalarial activity of the compounds in vitro, the parasites were cultured in Roswell Park Memorial Institute (RPMI) 1640 medium supplemented with 0.5 g/L L-glutamine, 5.96 g/L HEPES, 2 g/L sodium bicarbonate ($NaHCO_3$), 50 mg/L hypoxanthine, 10 mg/L gentamicin, 10% heat-inactivated human serum, and red blood cells (RBCs) at a 3% hematocrit in an atmosphere of 5% CO_2, 5% O_2, and 90% N_2 at 37 °C as previously described [26]. Ring-form parasites were collected using the sorbitol synchronization technique [27]. Briefly, the cultured parasites were collected by centrifugation at 840 g for 5 min at room temperature, suspended in a fivefold volume of 5% D-sorbitol (Nacalai Tesque, Kyoto, Japan) for 10 min at room temperature, and then they were washed twice with RPMI 1640 medium to remove the D-sorbitol. The utilization of blood samples of healthy Japanese volunteers for the parasite culture was approved by the institutional review committee of the Research Institute for Microbial Diseases (RIMD), Osaka University (approval number: 22-3).

Antimalarial activity

Ring-form-synchronized parasites were cultured with compounds **1**–**4** at sequentially decreasing concentrations (50, 15, 5, 1.5, 0.5, and 0.15 μM) for 48 h for the flow cytometric analysis using an automated hematology analyzer, XN-30. The XN-30 analyzer was equipped with a prototype algorithm for cultured falciparum parasites [prototype; software version: 01-03, (build 16)] and used specific reagents (CELLPACK DCL, SULFOLYSER, Lysercell M, and Fluorocell M) (Sysmex, Kobe, Japan) [28, 29]. Approximately 100 μL of the culture suspension diluted with 100 μL phosphate-buffered saline was added to a BD Microtainer MAP Microtube for Automated Process K_2 EDTA 1.0 mg tube (Becton Dickinson and Co., Franklin Lakes, NJ, USA) and loaded onto the XN-30 analyzer with an auto-sampler as described in the instrument manual (Sysmex). The parasitemia (MI-RBC%) was automatically reported [25]. Then 0.5% DMSO alone or containing 5 μM artemisinin was used as the negative and positive controls, respectively. The growth inhibition (GI) rate was calculated from the MI-RBC% according to the following equation:

$$\mathrm{GI}(\%) = 100 - (\text{test sample} - \text{positive control}) / (\text{negative control} - \text{positive control}) \times 100$$

The IC_{50} was calculated from GI (%) using GraphPad Prism version 5.0 (GraphPad Prism Software, San Diego, CA, USA) [30].

Supplementary Information The online version contains supplementary material available at https://doi.org/10.1007/s11418-023-01706-w.

Acknowledgements We thank Prof. Masatsugu Kimura (Osaka City University, Osaka, Japan) for the kind gift of the 3D7 strain, Mr. Yuji Toya and Dr. Kinya Uchihashi (Sysmex) for the setting of the XN-30 analyzer and Ms. Toshie Ishisaka and Ms. Sawako Itagaki for their technical assistance. This work was partly supported by JSPS KAKENHI (JP 19K07152 and JP 22K06671 to MH) and (JP 16K08309 to AEN), Japan.

References

1. Zhang Y, Xu H (2017) Recent progress in the chemistry and biology of limonoids. RSC Adv 7:35191–35220
2. Mohamad K, Hirasawa Y, Lim CS, Awang K, Hadi AHA, Takeya K, Morita H (2008) Ceramicine A and walsogyne A, novel limonoids from two species of Meliaceae. Tetrahedron Lett 49:4276–4278
3. Mohamad K, Hirasawa Y, Litaudon M, Awang K, Hadi AHA, Takeya K, Ekasari W, Widyawaruyanti A, Zaini NC, Morita H (2009) Ceramicine B-D, a new antiplasmodial limonoids from *Chisocheton ceramicus*. Bioorg Med Chem 17:727–730
4. Wong CP, Shimada M, Nagakura Y, Nugroho AE, Hirasawa Y, Kaneda T, Awang K, Hadi AHA, Mohamad K, Shiro M, Morita H (2011) Ceramicine E-I, new limonoids from *Chisocheton ceramicus*. Chem Pharm Bull 59:407–411
5. Wong C, Shimada M, Nugroho AE, Hirasawa Y, Kaneda T, Hadi AHA, Osamu S, Morita H (2012) Ceramicines J-L, new limonoids from *Chisocheton ceramicus*. J Nat Med 66:566–570
6. Nugroho AE, Hashimoto A, Wong C-P, Yokoe H, Tsubuki M, Kaneda T, Hadi AHA, Morita H (2018) Ceramicines M-P from *Chisocheton ceramicus*: isolation and structure–activity relationship study. J Nat Med 72:64–72
7. Wong CP, Deguchi J, Nugroho AE, Kaneda T, Hadi AHA, Morita H (2013) Ceramicines from *Chisocheton ceramicus* as lipid-droplets accumulation inhibitors. Bioorg Med Chem Lett 23:1786–1788
8. Wong CP, Kaneda T, Hadi AHA, Morita H (2014) Ceramicine B, a limonoid with anti-lipid droplets accumulation activity from *Chisocheton ceramicus*. J Nat Med 68:22–30
9. Iijima C, Wong CP, Nugroho AE, Sotozono Y, Someya S, Hirasawa Y, Kaneda T, Hadi AHA, Morita H (2016) Anti-melanin deposition activity of ceramicines from *Chisocheton ceramicus*. J Nat Med 70:702–707
10. Nugroho AE, Okuda M, Yamamoto Y, Hirasawa Y, Wong C-P, Kaneda T, Shirota O, Hadi AHA, Morita H (2013) Walsogynes B – G, limonoids from *Walsura chrysogyne*. Tetrahedron 69:4139–4145
11. Nugroho AE, Nakajima S, Wong C-P, Hirasawa Y, Kaneda T, Shirota O, Tougan T, Horii T, Hadi AHA, Morita H (2022) Walsogynes H – O from *Walsura chrysogyne*. J Nat Med 76:94–101
12. Prema WCP, Awouafack MD, Nugroho AE, Win YY, Win NN, Ngwe H, Morita H, Morita H (2019) Two new quassinoids and other constituents from the *Picrasma javanica* wood and their biological activities. J Nat Med 73:589–596
13. Prema WCP, Kodama T, Nugroho AE, El-Desoky AH, Awouafack MD, Win YY, Ngwe H, Abe I, Morita H, Morita H (2020) Three new quassinoids isolated from the wood of *Picrasma javanica* and their anti-Vpr activities. J Nat Med 74:571–578
14. Nugroho AE, Hirasawa Y, Kaneda T, Shirota O, Matsuno M, Mizukami H, Morita H (2021) Triterpenoids from *Walsura trichostemon*. J Nat Med 75:415–422
15. Nugroho AE, Tange M, Kusakabe Y, Hirasawa Y, Kaneda T, Shirota O, Matsuno M, Mizukami H, Tougan T, Horii T, Morita H (2022) Triterpenoids from *Walsura trichostemon*. J Nat Med 76:756–764
16. Nugroho AE, Zhang W, Hirasawa Y, Tang Y, Wong CP, Kaneda T, Hadi AHA, Morita H (2018) Bisleuconothines B-D, modified eburnane-aspidosperma bisindole alkaloids from *Leuconotis griffithii*. J Nat Prod 81:2600–2604
17. Nugroho AE, Ono Y, Jin E, Hirasawa Y, Kaneda T, Rahman A, Kusumawati I, Tougan T, Horii T, Zaini NC, Morita H (2021) Bisindole alkaloids from *Voacanga grandifolia* leaves. J Nat Med 75:408–414
18. Tang Y, Nugroho AE, Hirasawa Y, Tougan T, Horii T, Hamid A, Hadi A, Morita H (2019) Leucophyllinines A and B, bisindole alkaloids from *Leuconotis eugeniifolia*. J Nat Med 73:533–540
19. Amelia P, Nugroho AE, Hirasawa Y, Kaneda T, Tougan T, Horii T, Morita H (2019) Indole alkaloids from *Tabernaemontana macrocarpa* Jack. J Nat Med 73:820–825
20. Amelia P, Nugroho AE, Hirasawa Y, Kaneda T, Tougan T, Horii T, Morita H (2021) Two new bisindole alkaloids from *Tabernaemontana macrocarpa* Jack. J Nat Med 75:633–642
21. Hirasawa Y, Yasuda R, Minami W, Hirata M, Nugroho AE, Tougan T, Uchiyama N, Hakamatsuka T, Horii T, Morita H (2021) Divaricamine A, a new anti-malarial trimeric monoterpenoid indole alkaloid from *Tabernaemontana divaricata*. Tetrahedron Lett 83:153423
22. Hirasawa Y, Agawa-Kakimoto M, Zaima K, Uchiyama N, Goda Y, Morita H (2021) Complanadine F, a novel dimeric alkaloid from *Lycopodium complanatum*. J Nat Med 75:403–407
23. Hirasawa Y, Tanaka T, Hirasawa S, Wong CP, Uchiyama N, Kaneda T, Goda Y, Morita H (2022) Cliniatines A-C, new Amaryllidaceae alkaloids from *Clivia miniata*, inhibiting Acetylcholinesterase. J Nat Med 76:171–177
24. Ogasawara A, Noguchi R, Shigi T, Nugroho AE, Hirasawa Y, Kaneda T, Tougan T, Horii T, Hamid A, Hadi A, Morita H (2022) Caloforines A-G, coumarines from the bark of *Calophyllum scriblitifolium*. J Nat Med 76:645–653
25. Spartan'20 (2020) WaveFunction, Inc., Irvine, CA
26. Trager W, Jensen JB (1976) Human malaria parasites in continuous culture. Science 193:673–675. https://doi.org/10.1126/science.781840
27. Lambros C, Vanderberg JP (1979) Synchronization of *Plasmodium falciparum* erythrocytic stages in culture. J Parasitol 65:418–420
28. Tougan T, Suzuki Y, Itagaki S, Izuka M, Toya Y, Uchihashi K, Horii T (2018) An automated haematology analyzer XN-30 distinguishes developmental stages of falciparum malaria parasite cultured in vitro. Malar J 17:59. https://doi.org/10.1186/s12936-018-2208-6
29. Toya Y, Tougan T, Horii T, Uchihashi K (2021) Lysercell M enhances the detection of stage-specific Plasmodium-infected red blood cells in the automated hematology analyzer XN-31 prototype. Parasitol Int 80:102206. https://doi.org/10.1016/j.parint.2020.102206
30. Tougan T, Toya Y, Uchihashi K, Horii T (2019) Application of the automated haematology analyzer XN-30 for discovery and development of anti-malarial drugs. Malar J 18:8. https://doi.org/10.1186/s12936-019-2642-0